PHILOSOPHICAL TRANSACTIONS B

royalsocietypublishing.org/journal/rstb

Research

Cite this article: Graf A *et al*. 2020 Altered energy partitioning across terrestrial ecosystems in the European drought year 2018. *Phil. Trans. R. Soc. B* **375**: 20190524.
http://dx.doi.org/10.1098/rstb.2019.0524

Accepted: 3 July 2020

One contribution of 16 to a theme issue 'Impacts of the 2018 severe drought and heatwave in Europe: from site to continental scale'.

Subject Areas:
ecology, environmental science

Keywords:
eddy covariance, energy balance, evapotranspiration, heat flux, net carbon uptake, water-use efficiency

Author for correspondence:
Alexander Graf
e-mail: a.graf@fz-juelich.de

Electronic supplementary material is available online at https://doi.org/10.6084/m9.figshare.c.5105937.

THE ROYAL SOCIETY PUBLISHING

Altered energy partitioning across terrestrial ecosystems in the European drought year 2018

Alexander Graf[1], Anne Klosterhalfen[1,2], Nicola Arriga[3], Christian Bernhofer[4], Heye Bogena[1], Frédéric Bornet[5], Nicolas Brüggemann[1], Christian Brümmer[6], Nina Buchmann[7], Jinshu Chi[2], Christophe Chipeaux[8], Edoardo Cremonese[9], Matthias Cuntz[10], Jiří Dušek[11], Tarek S. El-Madany[12], Silvano Fares[13], Milan Fischer[11], Lenka Foltýnová[11], Mana Gharun[7], Shiva Ghiasi[7], Bert Gielen[14], Pia Gottschalk[15], Thomas Grünwald[4], Günther Heinemann[16], Bernard Heinesch[17], Michal Heliasz[18], Jutta Holst[18], Lukas Hörtnagl[7], Andreas Ibrom[19], Joachim Ingwersen[20], Gerald Jurasinski[21], Janina Klatt[22], Alexander Knohl[23], Franziska Koebsch[21], Jan Konopka[24], Mika Korkiakoski[25], Natalia Kowalska[11], Pascal Kremer[20], Bart Kruijt[26], Sebastien Lafont[8], Joël Léonard[5], Anne De Ligne[17], Bernard Longdoz[17], Denis Loustau[8], Vincenzo Magliulo[27], Ivan Mammarella[28], Giovanni Manca[3], Matthias Mauder[22], Mirco Migliavacca[12], Meelis Mölder[18], Johan Neirynck[29], Patrizia Ney[1], Mats Nilsson[2], Eugénie Paul-Limoges[30], Matthias Peichl[2], Andrea Pitacco[31], Arne Poyda[20,32], Corinna Rebmann[33], Marilyn Roland[14], Torsten Sachs[15], Marius Schmidt[1], Frederik Schrader[6], Lukas Siebicke[23], Ladislav Šigut[11], Eeva-Stiina Tuittila[34], Andrej Varlagin[35], Nadia Vendrame[31], Caroline Vincke[36], Ingo Völksch[22], Stephan Weber[24], Christian Wille[15], Hans-Dieter Wizemann[37], Matthias Zeeman[22] and Harry Vereecken[1]

[1]Institute of Bio- and Geosciences: Agrosphere (IBG3), Forschungszentrum Jülich, Wilhelm-Johnen-Straße, 52428 Jülich, Germany
[2]Department of Forest Ecology and Management, Swedish University of Agricultural Sciences, Skogsmarksgränd 17, 90183 Umeå, Sweden
[3]European Commission, Joint Research Centre (JRC), Ispra, Italy
[4]Chair of Meteorology, Technische Universität Dresden, Pienner Straße 23, 01737 Tharandt, Germany
[5]BioEcoAgro Joint Research Unit, INRAE, Université de Liège, Université de Lille, Université de Picardie Jules Verne, 02000 Barenton-Bugny, France
[6]Institute of Climate-Smart Agriculture, Johann Heinrich von Thünen Institute, Bundesallee 65, 38116 Braunschweig, Germany
[7]Department of Environmental Systems Science, ETH Zurich, Universitätstraße 2, 8092 Zurich, Switzerland
[8]ISPA, Bordeaux Sciences Agro, INRAE, 33140, Villenave d'Ornon, France
[9]Climate Change Unit, Environmental Protection Agency of Aosta Valley, Italy
[10]Unité mixte de Recherche Silva, Université de Lorraine, AgroParisTech, INRAE, UMR Silva, 54000 Nancy, France
[11]Department of Matter and Energy Fluxes, Global Change Research Institute of the Czech Academy of Sciences, Bělidla 986/4a, 60300 Brno, Czech Republic
[12]Department of Biogeochemical Integration, Max Planck Institute for Biogeochemistry, Hans-Knöll-Straße 10, 07745 Jena, Germany
[13]National Research Council (NRC), Institute of Bioeconomy, Via dei Taurini 19, 00100 Rome, Italy
[14]University of Antwerp, Plants and Ecosystems, Universiteitsplein 1, 2610 Wilrijk, Belgium
[15]Remote Sensing and Geoinformatics, German Research Centre for Geosciences (GFZ), Telegrafenberg, 14473 Potsdam, Germany
[16]Environmental Meteorology, University of Trier, Behringstraße 21, 54296 Trier, Germany
[17]Terra Teaching and Research Centre, University of Liege – Gembloux Agro-Bio Tech, Avenue de la Faculté, 8, 5030 Gembloux, Belgium

[18]Department of Physical Geography and Ecosystem Science, Lund University, Sölvegatan 12, 22362 Lund, Sweden
[19]Department of Environmental Engineering, Technical University of Denmark (DTU), Bygningstorvet 115, 2800 Lyngby, Denmark
[20]Institute of Soil Science and Land Evaluation, University of Hohenheim, Emil-Wolff-Straße 27, 70599 Stuttgart, Germany
[21]Department for Landscape Ecology and Site Evaluation, University of Rostock, Justus von Liebig Weg 6, 18059 Rostock, Germany
[22]Institute of Meteorology and Climate Research - Atmospheric Environmental Research, Karlsruhe Institute of Technology, Campus Alpin, Kreuzeckbahnstraße 19, 82467 Garmisch-Partenkirchen, Germany
[23]Bioclimatology, University of Göttingen, Büsgenweg 2, 37077 Göttingen, Germany
[24]Climatology and Environmental Meteorology, Institute of Geoecology, Technische Universität Braunschweig, Langer Kamp 19c, 38106 Braunschweig, Germany
[25]Climate System Research Unit, Finnish Meteorological Institute, PO Box 503, 00101 Helsinki, Finland
[26]Department of Environmental Sciences, Wageningen University and Research, PO Box 47, 6700 AA Wageningen, The Netherlands
[27]CNR - Institute for Agricultural and Forest Systems, Via Patacca, 85, 80040 Ercolano (Napoli), Italy
[28]Institute for Atmospheric and Earth System Research/Physics, Faculty of Science, University of Helsinki, Gustaf Hällströmin katu 2B, 00014 Helsinki, Finland
[29]Research Institute for Nature and Forest, INBO, Havenlaan 88 Box 73, 1000 Brussels, Belgium
[30]Department of Geography, University of Zurich, Winterthurerstraße 190, 8057 Zurich, Switzerland
[31]Department of Agronomy, Food, Natural resources, Animals and Environment, University of Padova, Viale dell'Università 16, 35020 Legnaro, Italy
[32]Institute of Crop Science and Plant Breeding, Grass and Forage Science/Organic Agriculture, Christian-Albrechts-University Kiel, Hermann-Rodewald-Straße 9, 24118 Kiel, Germany
[33]Helmholtz Centre for Environmental Research GmbH - UFZ, Department Computational Hydrosystems, Permoserstraße 15, 04318 Leipzig, Germany
[34]School of Forest Sciences, University of Eastern Finland, Yliopistokatu 7, 80101 Joensuu, Finland
[35]Laboratory of Biocentology, A.N. Severtsov Institute of Ecology and Evolution, Russian Academy of Sciences, Leninsky pr.33, Moscow 119071, Russia
[36]Environmental Sciences, Earth and Life Institute, Université catholique de Louvain, 1348 Louvain-la-Neuve, Belgium
[37]Institute of Physics and Meteorology, University of Hohenheim, 70593 Stuttgart, Germany

AG, 0000-0003-4870-7622; AKl, 0000-0001-7999-8966; NBr, 0000-0003-3851-2418; CBr, 0000-0001-6621-5010; NBu, 0000-0003-0826-2980; JC, 0000-0001-5688-8895; CC, 0000-0003-0338-8517; EC, 0000-0002-6708-8532; MC, 0000-0002-5966-1829; TSE-M, 0000-0002-0726-7141; LF, 0000-0001-8202-955X; MG, 0000-0003-0337-7367; TG, 0000-0003-2263-0073; GH, 0000-0002-4831-9016; BH, 0000-0001-7594-6341; JH, 0000-0001-8719-1927; LH, 0000-0002-5569-0761; AI, 0000-0002-1341-921X; GJ, 0000-0002-6248-9388; AKn, 0000-0002-7615-8870; FK, 0000-0003-1045-7680; MK, 0000-0001-6875-9978; NK, 0000-0002-7366-7231; SL, 0000-0002-9605-8092; JL, 0000-0002-9907-9104; DL, 0000-0003-3990-400X; VM, 0000-0001-5505-6552; IM, 0000-0002-8516-3356; MMa, 0000-0002-8789-163X; MMi, 0000-0003-3546-8407; PN, 0000-0001-6821-8661; MP, 0000-0002-9940-5846; APi, 0000-0002-7260-6242; CR, 0000-0002-8665-0375; MR, 0000-0002-5770-3896; TS, 0000-0002-9959-4771; MS, 0000-0001-5292-7092; FS, 0000-0002-5668-3467; LŠ, 0000-0003-1951-4100; AV, 0000-0002-2549-5236; NV, 0000-0002-2772-6755; IV, 0000-0001-9700-2771; SW, 0000-0003-0335-4691; MZ, 0000-0001-9186-2519; HV, 0000-0002-8051-8517

Drought and heat events, such as the 2018 European drought, interact with the exchange of energy between the land surface and the atmosphere, potentially affecting albedo, sensible and latent heat fluxes, as well as CO_2 exchange. Each of these quantities may aggravate or mitigate the drought, heat, their side effects on productivity, water scarcity and global warming. We used measurements of 56 eddy covariance sites across Europe to examine the response of fluxes to extreme drought prevailing most of the year 2018 and how the response differed across various ecosystem types (forests, grasslands, croplands and peatlands). Each component of the surface radiation and energy balance observed in 2018 was compared to available data per site during a reference period 2004–2017. Based on anomalies in precipitation and reference evapotranspiration, we classified 46 sites as drought affected. These received on average 9% more solar radiation and released 32% more sensible heat to the atmosphere compared to the mean of the reference period. In general, drought decreased net CO_2 uptake by 17.8%, but did not significantly change net evapotranspiration. The response of these fluxes differed characteristically between ecosystems; in particular, the general increase in the evaporative index was strongest in peatlands and weakest in croplands.

This article is part of the theme issue 'Impacts of the 2018 severe drought and heatwave in Europe: from site to continental scale'.

1. Introduction

Exceptionally dry and warm periods can serve as a testbed for the future response of the land surface to climate change, as they represent air temperature, net radiation (R_n) and regionally also precipitation (P) and incident solar radiation (R_{si}) levels that may occur more frequently in the future. Depending on their severity and duration, heatwave and soil water shortage episodes have been observed to dramatically reduce plant productivity, ecosystems' carbon balance and food, fibre and wood production in Europe, with an increasing frequency during the three last decades [1–3]. In contrast with distinct summer heatwaves, in 2018, unusually warm conditions throughout most of Europe and dry conditions in its northern half started in spring and persisted throughout the remainder of the year [4], representing the largest annual soil moisture anomaly in the period 1979–2019 [5].

Higher R_n enforces an increase in the sum of the turbulent sensible heat flux (H), latent heat flux (λET), heat stored in the ground, vegetation and water bodies (S_l) and energy converted chemically (E_c), particularly into biomass by photosynthetic CO_2 uptake or vice versa by respiration:

$$H + \lambda\mathrm{ET} + S_l + E_c = R_n = (1-\alpha)R_{si} - R_{lo} + R_{li}. \quad (1.1)$$

Land surface albedo (α), outgoing longwave radiation from the land surface (R_{lo}) and incoming longwave radiation from the atmosphere (R_{li}) co-determine the relation between R_{si} and R_n.

A small increment in R_n can increase any, and probably all, terms on the left-hand side of equation (1.1). If sunny and dry conditions prevail, however, changes will be more diverse. The increase in E_c may diminish as photosynthesis becomes limited by stomatal closure or biochemical limitations [6]. The same may happen to evapotranspiration (ET) as near-surface water for evaporation becomes depleted or stomatal closure limits transpiration. As stomatal closure or soil water shortage continues, plants may develop less green leaf area than usual or initiate senescence, eventually leading to a decrease in transpiration and E_c, as well as to a change in α and thus R_n. At the same time, soil water shortage can reduce soil respiration

in spite of higher temperature, moderating the decrease in E_c, as shown for the 2003 drought and heatwave [1,2]. If a warm anomaly is characterized by advection rather than by local production of atmospheric heat, H might decrease according to the temperature difference between land surface and atmosphere. Hence, responses on the left-hand side of equation (1.1) might differ in magnitude and sign between fluxes.

The objective of this study was to analyse the response of land surface–atmosphere energy fluxes to the exceptionally dry and warm conditions during the year 2018 at ecosystem monitoring sites across Europe. Based on the response mechanisms described above, we hypothesize that S_l and H are likely to consistently increase across different ecosystems. ET and E_c, by contrast, may increase in response to increasing R_n and R_{si}, respectively, or decrease in response to soil water depletion. ET and E_c are linked to each other by the drought response of the vegetation, but can partly decouple owing to the role of soil respiration and evaporation. Each flux has a different effect on the atmosphere, e.g. direct heating through H, local cooling and nonlocal heating through ET, and long-term global cooling through the greenhouse effect of E_c on R_{li}. Examining the ecosystem-dependent variability of ET and E_c responses, and their side effect on H, may help to understand how land use modulates local and global heating in response to droughts and heatwaves [7]. In this study, we compared fluxes from equation (1.1) directly measured at 56 eddy covariance [8] stations across Europe in 2018 to those in a reference period 2004–2017, discriminating between the ecosystem types forest, grassland, cropland and peatland.

2. Methods

Meteorological data and fluxes [9] were originally provided as half-hourly averages, mostly in the framework of the ICOS (www.icos-ri.eu) and TERENO (www.tereno.net) networks [10,11]. A site was selected for this study when sufficient data of the turbulent fluxes of sensible heat, water vapour and CO_2 were available for 2018 and at least for one year from the reference period 2004 to 2017. All 14 reference years were available at seven sites, and only one reference year at four sites. The majority of sites were forest sites, 10 were crop sites, nine grassland sites and six peatland sites (electronic supplementary material, (*a*), table S1 for details). Reference years with incomparable land use to 2018 (e.g. different crops in a crop rotation, or years before wood harvesting) were omitted and are already excluded from the above numbers.

While all radiation terms of equation (1.1) were measured directly and the turbulent fluxes were computed from high-frequency raw data [11–13], S_l and E_c were estimated according to:

$$E_c \approx -0.469 \frac{J}{\mu\text{mol}} \text{NEE} \tag{2.1}$$

and

$$S_l \approx \text{SHF}_d + d(\overline{\rho_s}\,\overline{c_s} + \overline{\theta_w}\rho_w\, c_w)\frac{\Delta\overline{T_s}}{\Delta t} + \frac{m_c}{A}\overline{c_c}\frac{\Delta\overline{T_c}}{\Delta t} + h_m\left(\overline{\rho_a}c_p\frac{\Delta\overline{T_a}}{\Delta t} + \lambda\frac{\Delta\overline{\rho_v}}{\Delta t}\right). \tag{2.2}$$

Note that in equation (2.1), past studies on energy balance closure (EBC) used different CO_2 flux components such as net ecosystem exchange (NEE), gross primary production (GPP) or overstorey CO_2 flux to estimate E_c, which typically contributes ≪5% to the budget [14–18]. The measurement or modelling technique for the different components of S_l (equation (2.2)) determines whether heat released by respiration needs to be excluded, included or partly included in equation (2.1). In most cases including this study, the unknown fraction of (soil) respiration below level d (equation (2.2)) would need to be excluded. By estimating E_c from NEE, we avoid overestimating energy balance closure and inducing further uncertainties from source partitioning. This also implies relative changes in E_c reported in this study are equivalent to relative changes in net carbon uptake (ecosystem productivity) NEP = −NEE.

The soil heat flux at depth d (SHF_d) is measured by heat flux plates (first term on the right-hand side of equation (2.2)) and corrected for estimated storage changes over time ($\Delta/\Delta t$) between plate and soil surface (second term), in biomass (third term) and air below the flux measurement level (last term). They depend on temperature (T), density (ρ) and specific heat capacity (c) of the respective medium soil (s), soil water (w, θ_w being the volumetric soil water content), plant canopy (c, $m_c\ A^{-1}$ being wet biomass per unit area), air (a) and water vapour (v, c_p being atmospheric heat capacity at constant pressure and λ the water vaporization enthalpy). In each term, the height integral was approximated by multiplying average available measurement values (indicated by overbars, see the electronic supplementary material, (a) for details) with the respective layer thickness d and h_m (height of flux level).

The combined inter-annual and spatial variability of the change of a variable in 2018 versus the reference period was used to estimate its 95% confidence interval (more details in the electronic supplementary material, (a)). We report only changes that were significant against this variability, unless explicitly stated otherwise.

For the water budget and drought intensity, the potential evapotranspiration (ET in absence of water stress) is an important characteristic, which can be estimated by the Penman–Monteith equation. To disentangle atmospheric conditions from site-specific responses and to rely on variables available with high temporal coverage and quality at all sites, we used the grass reference evapotranspiration ET_0 [19]. A meteorological, atmospheric or potential drought is defined by either the anomaly in precipitation (ΔP), or in the climatological water balance (P - ET_0) [20–22]. Obviously, the latter definition captures more of the processes that can eventually lead to actual drought stress or soil drought. However, not all of ET_0 leads to actual water loss by ET at each site, and ET_0 also correlates with factors positively affecting plant growth in energy-, temperature- or light-limited regions, such as R_{si} or growing degree days. Therefore, figures 1 and 2 depict all sites in a two-dimensional coordinate system of both ΔP and ΔET_0.

3. Results and discussion

(a) Meteorological drought conditions

In 2018, most sites (46 of 56) were characterized by a joint negative ('dry') ΔP, positive ('dry') ΔET_0, and $\Delta(P - \text{ET}_0)$ below −75 mm (lower right quadrant of figure 1*a*). This group of sites, which suffered atmospheric drought conditions according to any of these three definitions on an annual basis, will be referred to as *affected* sites. It includes 26 forest, seven crop, seven grassland and six peatland sites. While ΔP in this group spanned a large range of more than 500 mm, ΔET_0 was confined to a narrow band around +100 mm. On average, P was reduced by 180 mm and ET_0 increased by 105 mm. Mean annual temperature across these sites was 0.82°C higher than in the reference period, with little variability among ecosystem types except for peatlands, which showed only 0.66°C average increase and a comparatively large variability among sites (see the electronic

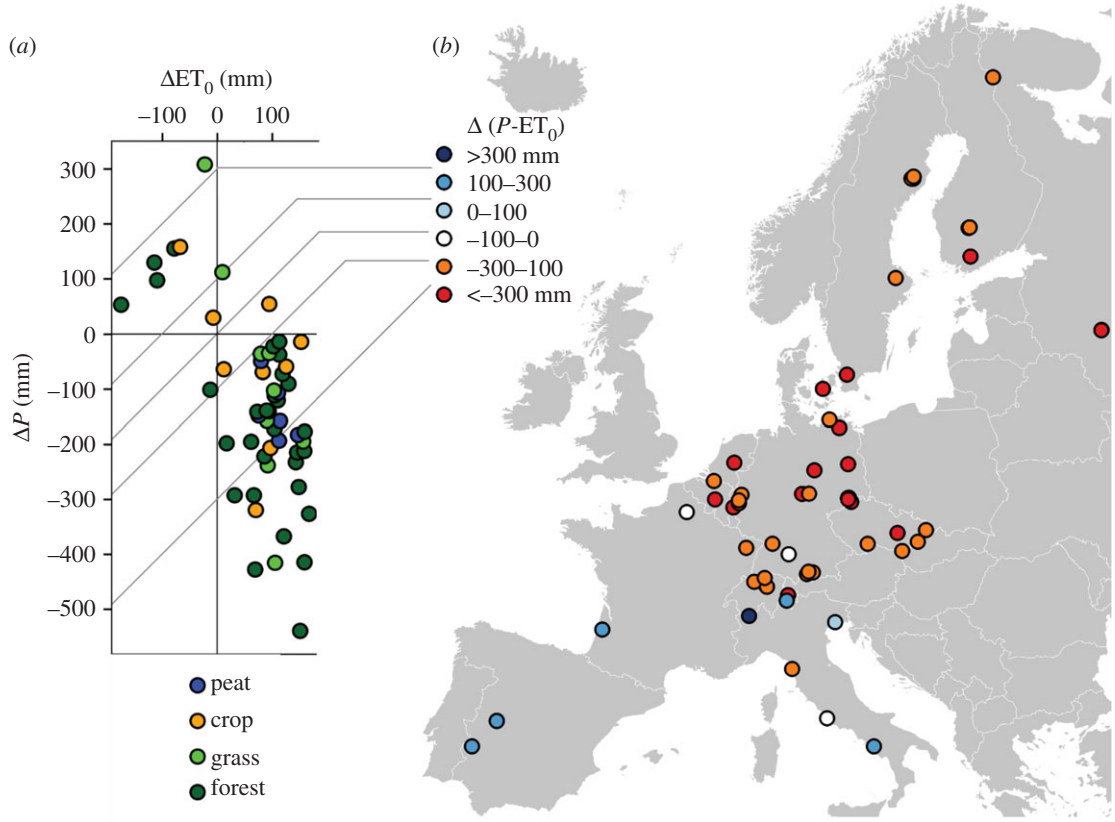

Figure 1. 2018 anomalies in precipitation (P) and grass reference evapotranspiration (ET_0); (*a*) by ecosystem type, diagonal broken lines correspond to P-ET_0 anomalies in steps of 100 mm; and (*b*) by location, colours refer to bins of P-ET_0 anomalies.

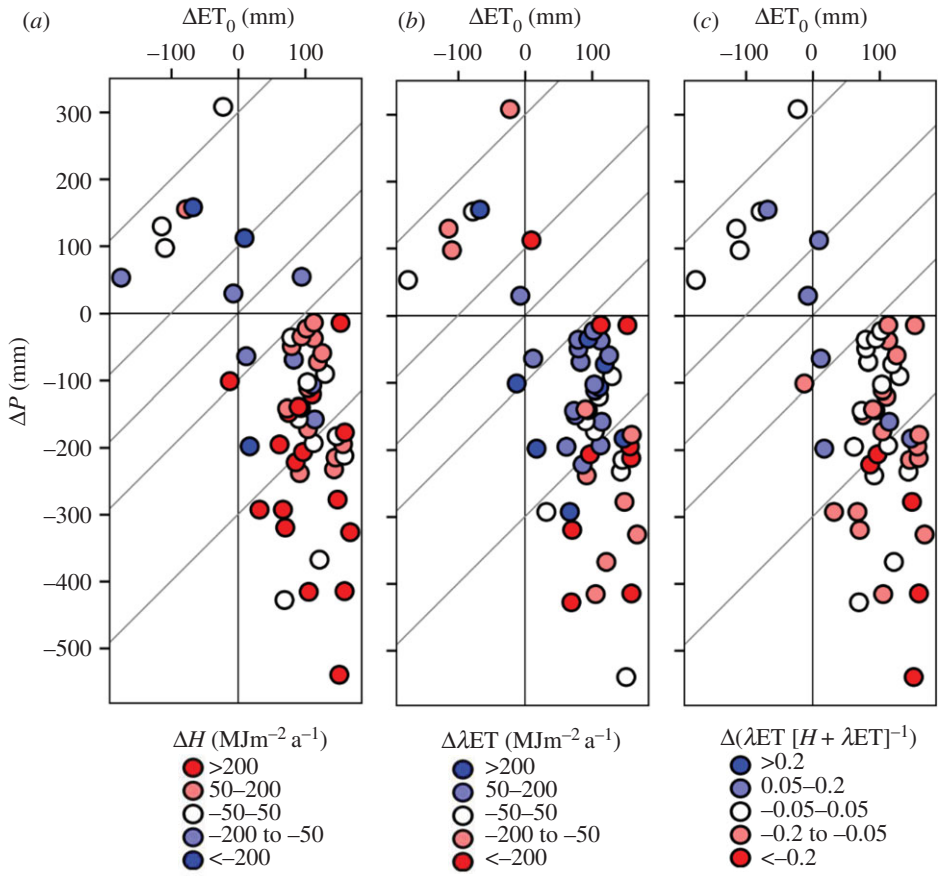

Figure 2. Annual 2018 anomalies of sensible heat flux (H) (*a*), latent heat flux (λET) (*b*), and evaporative fraction ($\lambda ET\ (H + \lambda ET)^{-1}$) (*c*) as a function of precipitation P and grass reference ET_0 deficits. Diagonal isolines indicate P-ET_0 anomalies of 0, ±100 and ±300 mm (figure 1).

supplementary material, (*a*), table S2). The remaining smaller group of 10 sites, referred to as *other*, included few sites with a moderate $\Delta(P - ET_0)$ deficit of less than 100 mm, and potential drought stress eminent only in ΔP or ΔET_0, but not both. The majority of this group, which may or may not have suffered drought conditions during subperiods of 2018, exhibited positive ('wet') annual P anomalies jointly with negative ('wet') ET_0 anomalies. ΔET_0 was thus (negatively) correlated to ΔP ($r = -0.60$), and by its role in the Penman–Monteith equation positively to R_{si} ($r = 0.87$), but also to the sum of growing degree days above 10°C ($r = 0.78$), which is potentially beneficial for plant growth. Flux site data thus confirm that over a large region of Europe, 2018 was not a singular rain-deficient, warm, or sunny year, but showed a combination of these anomalies. *Affected* sites were located in central Europe north of the Alps, Scandinavia and Eastern Europe (figure 1*b*), in general agreement with other ground-based and remote sensing observations as well as models [21,23]. In particular, affected sites are well distributed across the region suffering the strongest annual reduction in the standardized precipitation-evapotranspiration index (SPEI [24]).

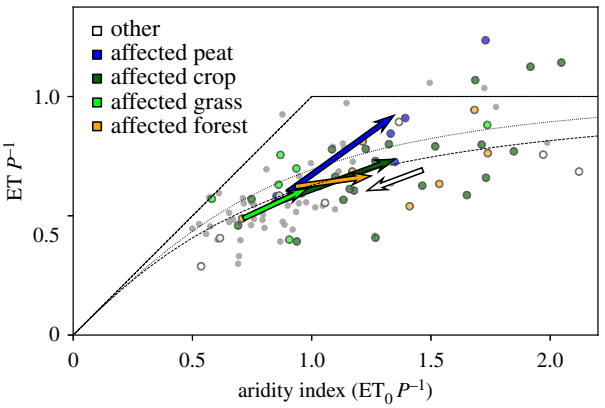

Figure 3. Budyko plot of the evaporative index (ET P^{-1}) versus the aridity index (ET_0 P^{-1}). Arrows show the mean shift of annual ratios between the reference period and 2018 (arrow head), averaged per *affected* ecosystem type and over all *other* sites. Circles indicate the ratios for each single site (coloured: in 2018, small grey: reference period, axes clipped owing to maxima of ET_0 P^{-1} and ET P^{-1} of 4.3 and 1.8, respectively). Dotted straight lines: theoretical energy (1 : 1 line) and water (horizontal) limits; grey line: expected ensemble behaviour after [28]; broken line: fit from [29] to FLUXNET data not corrected for energy balance closure.

(b) Changes in radiation balance and energy balance closure

Incoming shortwave (global solar) radiation (R_{si}) across *affected* sites increased by +360 MJ m^{-2} yr^{-1} (+9%), as opposed to −147 MJ m^{-2} yr^{-1} across the *other* sites. Radiation budget components other than R_{si} were not available with sufficient coverage at all sites, such that the following results represent sub-datasets (see the electronic supplementary material, (*a*), table S2, minimum 35 *affected* and six *other* sites).

Outgoing shortwave radiation (R_{so}) was mostly following incoming radiation R_{si}, increasing slightly more (+11.5%), most likely owing to a small net albedo change, which was however not significant, differing in sign between ecosystems and sites.

Incoming longwave radiation at *affected* sites changed insignificantly (+24 MJ m^{-2} yr^{-1}, +0.2%, but +1.6% at *other* sites), indicating cancelling effects of increased atmosphere temperature (positive) and reduced cloudiness (negative). Outgoing longwave radiation, by contrast, reflected the higher land surface temperature at *affected* sites (148 MJ m^{-2} yr^{-1}, +1.3%) in comparison to no significant change at *other* sites.

Net radiation (R_n) changed by +123 MJ m^{-2} yr^{-1} (+6.3%) across *affected* while not significantly across *other* sites, reflecting the dominant role of R_{si} and the moderating role of higher outgoing longwave radiation from the warmer land surface. However, a large variability (95% confidence interval ±60 MJ m^{-2} yr^{-1}) might indicate instrumental issues at some sites.

Eddy covariance measurements are known for a gap in the EBC, i.e. the sum of H and λET is frequently 15 to 30% smaller than $R_n - S_l - E_c$ [25,26]. Mean EBC across sites in this study changed by 3% between the reference period and 2018 (see electronic supplementary material, (b) for details), indicating that relative changes in the fluxes reported remain independent of the EBC problem. Owing to the ongoing debate about its reasons and implications for any hypothetical flux correction, absolute fluxes are reported without any correction [27] for the EBC gap, which was on average 20% in our study.

(c) Sensible heat and evapotranspiration

Among the non-radiative surface energy fluxes (left-hand side of equation (1.1)), the sensible heat flux (H) showed the strongest and most consistent change across *affected* sites, with +169 MJ m^{-2} yr^{-1} (+32.3%, and no significant change across *other* sites, figure 2*a*).

Latent heat flux at *affected* sites did not change significantly on average (−0.3 MJ m^{-2} yr^{-1}). We attribute this to the opposing roles of increased ET_0 on the one hand and soil water depletion, stomatal closure and plant development on the other hand. ET increased where and when sufficient water was available from recent precipitation or from long-term storage, and later decreased only at sites where stored soil water was depleted (electronic supplementary material, (c)). Consequently, among *affected* sites annual λET typically decreased at those sites with a severe precipitation deficit, while it frequently increased at sites with the same ET_0 surplus but only moderate precipitation deficit (figure 2*b*). Figure 2*c* shows a clearer drought signal in the evaporative fraction (fraction of H+λET used for ET): even where ET increased, it typically increased less than proportionally to the larger energy available.

Averages across ecosystems further confirm this hypothesis of ET response depending on stored water. *Affected* peatland sites were the only ecosystem type with a significant increase in λET (+205 MJ m^{-2} yr^{-1}) and no significant increase in H. Crop sites showed a significant decrease in λET (−122 MJ m^{-2} yr^{-1}), which could have a number of reasons: (i) crop sites are under-represented among high elevation and high latitude sites, thus water limitation at a given precipitation deficit is more likely compared to some forest and grassland sites at higher elevations or latitudes; (ii) crop sites typically feature periods of bare soil, during which ET is dominated by evaporation. Transpiration can be sustained longer than evaporation because of the access of plants roots to water in deeper soil layers; (iii) these periods may start earlier in a drought year owing to accelerated maturity and harvest (electronic supplementary material, (c)).

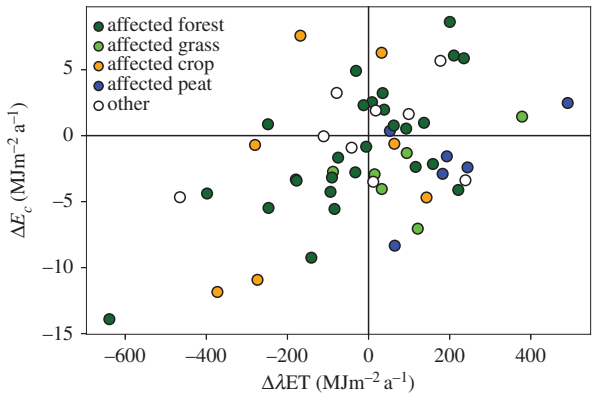

Figure 4. 2018 annual anomalies in energy used for CO_2 uptake (E_c), versus energy used for evapotranspiration (λET) ($r = 0.49$, reduced major axis slope = 0.023).

In 2018, anomalies in ET of grassland, forest and *other* sites reacted to ET_0 and P as predicted by the Budyko framework ([28], figure 3). A small offset may reflect a systematic underestimation of ET owing to the EBC and vanishes when comparing to the curve fit by Williams *et al.* [29]. At crop sites, however, the fraction of P used for ET increased less, as could be expected according to the above reasons. All six peatland sites showed an increase in ET, which was linearly related to the increase in ET_0. One of them (DE-SfS) is an ombrogenic bog fed only by precipitation and showed the smallest ET increase and largest H increase among peatland sites. The remaining fen peatlands can receive additional inflows from the surrounding landscape and increase ET in response to higher ET_0 and lower P for a longer period than other ecosystems. Bogs show a vertical pore space structure and self-regulatory mechanisms [30] that could lead to an earlier decrease in ET. A few peatland and forest sites lost more water by ET than they received by P (points above the water limit line in figure 3). At one peatland site (DE-ZRK), available measurements of the change in water table depth between the start and the end of 2018 (−0.65 m) would reconcile ET P_{2018}^{-1} (1.8, not shown in figure 3 for scaling reasons) with the theoretical water limit. A detailed analysis of the effect of extractable soil water in forests for selected sites is presented in [6].

On an annual basis, *affected* forest sites showed a larger average increase in H (+235 MJ m^{-2} yr^{-1}) than grassland sites (+79 MJ m^{-2} yr^{-1}), while the contrast in the insignificant ET changes between both ecosystems was opposite. For the case of 2003, it was demonstrated [7] that owing to differences in stomatal control and rooting depth, forests show less ET and more H than grasslands during the early stage of a heatwave. Ultimately, however, the resulting more rapid depletion of available soil water under grass led to more atmospheric heating than over forests at the peak of the heatwave 2003 [7]. Evolutionary reasons for such a more conservative strategy of forests are suggested in [31]. According to our study, the former effect (more heating over forests) dominated over the latter (more heating over grasslands once soil water is depleted) on an annual basis in 2018. This may be partly owing to the lower albedo resulting in higher total available energy of forests, partly owing to the grassland ensemble including more humid sites (figure 3), and partly to the different timescales of the studies. A brief sub-annual comparison between grasslands and forests largely supporting [7] is presented in the electronic supplementary material, (c). Also for 2003, an analysis of four example catchments showed a net increase of ET [32] to amplify the soil drought, which could not be found at the majority of our sites on an annual basis in 2018. However, as a consequence of more available energy transferred as H, apart from direct heating of the atmosphere, precipitation can also be reduced owing to a higher and cooler cloud base [33].

(d) Minor energy fluxes, water-use efficiency of CO_2 uptake and soil water content

The increase in heat storage in the soil and the canopy was small (+9 MJ m^{-2} yr^{-1} across *affected* sites), demonstrating that most of the additional energy during a warm and dry anomaly is transferred back to the atmosphere. The relative change was large (approx. 300%) owing to the fact that net energy storage was approximately balanced in the reference period.

The change in energy storage in photosynthesis products was even smaller and highly variable between sites (−1.6 MJ m^{-2} yr^{-1} across *affected*, insignificant across *other* sites). However, the change across *affected* sites corresponds to 17.8% of reference period CO_2 uptake, or 38 g C m^{-2} yr^{-1}. The radiative forcing of this amount not removed from the atmosphere in 2018, estimated according to the methodology of [34] and [35], corresponds to 1.9 MJ m^{-2} yr^{-1} during each year of its atmospheric lifetime, such that the total heating effect owing to unused photosynthetic energy and the greenhouse effect cumulates to, e.g. 3.5 MJ m^{-2} yr^{-1} in 2019. Our observation of a reduced net CO_2 uptake across *affected* sites is in general agreement with observed changes in atmospheric CO_2 concentrations over Europe [36,37].

CO_2 uptake is typically closely related to ET loss through the concept of water-use efficiency [38,39]. Inherent water-use efficiency (IWUE*) estimated from annual GPP, vapour pressure deficit and ET according to Beer *et al.* [40] increased across *affected* sites by 3.1 g C hPa kg^{-1} H_2O (31.4%, no significant change across *other* sites). For assessing the climatological response of the land surface to drought, it is worthwhile to also consider the net ecosystem water-use efficiency −NEE ET^{-1} (WUEeco) or, dimensionless, E_c λET^{-1}. While CO_2 uptake adds to the potential of an ecosystem to mitigate drought and heatwaves in any respect (see above), ET has ambiguous effects, providing a local cooling and moistening of the atmosphere on the one hand, while on the other hand transferring latent heat to the atmosphere, adding H_2O to its greenhouse gas concentration at least on a short term, and depleting soil water needed for future productivity. E_c λET^{-1} decreased across *affected* sites by $-11 \cdot 10^{-4}$ (−13.8%, no significant change across *other* sites). On average, the affected land surface thus reinforced water scarcity and global warming during the drought and heatwave. Soil water content measured within the top 0.3 m of the soil decreased on average by −0.05 cm^3 cm^{-3} (−16.2%), while increasing by 0.03 cm^3 cm^{-3} across *other* sites. Differences between forest and grassland sites in both IWUE* and WUEeco (electronic supplementary material, (*a*), table S2) are in qualitative agreement with a forest–grassland comparison among Swiss sites, where forest significantly increased water-use efficiency [31]. However, figure 4 demonstrates that the relationship between smaller CO_2 uptake and increased ET water loss [2] was not universal. Peatlands typically lost more water via ET than in the reference period without absorbing more CO_2, possibly because of exposure of large amounts of organic carbon in otherwise

inundated soils to aerobic conditions favouring respiration, or an increase in evaporation rather than transpiration. Some of the *affected* cropland and forest sites, in contrast, showed increased CO_2 uptake with no or little additional water loss. A more detailed future analysis of the site-specific conditions causing such responses might help to develop more drought- and warming-resilient land-use strategies.

4. Conclusion

Among the land surface responses to the 2018 European drought, a considerable relative increase in H by 32.3% was the most important change in absolute terms, as well as the most consistent one across ecosystem types and drought intensities. λET did not change significantly on average but showed a large variability, including increases at sites with large water reservoirs (peatlands) or moderate drought intensity and stronger decreases at crop sites. However, the evaporative fraction (fraction of turbulent heat transfer used for λET) clearly decreased and the evaporative index (fraction of precipitation used for λET) clearly increased across ecosystems. Responses in energy used for net CO_2 uptake (E_c) showed a correspondingly large variability and a moderate correlation to λET response, but a significant average decrease of −17.8%. Heat storage in the ground showed a strong relative but small absolute increase, and the response of albedo was variable, generally small and as a result not significant across the assessed sites.

Albedo and E_c potentially cool the land surface–atmosphere system, the latter both through energy consumption during photosynthesis and greenhouse gas removal, while H has a heating effect. λET has a large variety of effects including local cooling and nonlocal heating of the atmosphere, atmospheric humidity and cloud formation, and depletion of water resources required for productivity and groundwater recharge. Thus, an increase or decrease in ET does not generally mitigate or reinforce drought, but must be assessed considering local priorities and potential correlations with E_c and albedo. Because H increased consistently, CO_2 uptake decreased on average and albedo and ET showed no consistent change, the affected European land surface responded with a clear net heating effect to the drought in 2018.

Data accessibility. This study is mainly based on the dataset: https://doi.org/10.18160/YVR0-4898. Data of additional sites and missing single variables for some sites have been obtained directly from the institutions and are available from the data repositories of these institutions. The corresponding author can provide the respective institutional contact or repository on request.

Authors' contributions. A.G., A.Kl., C.Br., C.R., F.S. and H.V. conceived the study. A.G. and A.Kl. assembled the database, designed the scripts and figures, and carried out the analysis, with input from all other authors. A.G. wrote the manuscript with input from all authors. All authors read, corrected and approved the submitted version of the manuscript. Analysis of raw data from each site towards half-hourly averages and fluxes, planning and quality assurance of the sites was provided by all authors.

Competing interests. We declare we have no competing interests.

Funding. Authors thank the funders (grant IDs and particularly concerned authors/sites in parentheses) French National Research Agency ANR (ANR-11-LABX-0002-01, ANR-16-SUMF-0001-01, LabEx ARBRE, M.C.), Alexander von Humbold Stiftung (MaNiP, T.S.E.-M., M.Mi.), German Federal Ministry of Education and Research BMBF (01LN1313A, A.G.; ICOS; DE-Geb), German Federal Ministry of Food and Agriculture BMEL (ERA-NET FACCE ERA-GAS, P.G., F.S., C.Br.), German Research Foundation DFG (BE1721/23, C.Be., T.G., DE-Tha; PAK 346; FOR 1695, A.P., J.I., H.W., DE-EC2, DE-EC4; INST 186/1118-1 FUGG, A.Kn., L.S.), GIP Ecofor SOERE F-ORE-T (M.C.), Finnish Center of Excellence (307331, I.M.), Research Foundation-Flanders FWO (BE-Bra; G0H3317N, B.G.), Hainich National Park (DE-Hai), Helmholtz Association HGF (TERENO; VH-NG-821, T.S.), Horizon 2020 (696356, P.G.), ICOS-FINLAND (281255, I.M.), Kempe Foundation (SMK-1743, J.C.), Knut and Alice Wallenberg Foundation (2015.0047, M.P.), Max-Planck Institute for Biogeochemistry (DE-Geb), Russian Foundation for Basic Research RFBR (19-04-01234-a, A.V.), Swiss National Science Foundation (ICOS-CH Phase 2 20FI20_173691, M.G., N.Bu.; InnoFarm 407340_172433, N.Bu.), European Commission (SUPER-G, S.G.; RINGO, L.H.; ERA-NET Sumforest No. 606803, M.C.), Service Public de Wallonie (DGO6, 1217769, A.D.L., B.H., B.L., C.V.), SustES (CZ.02.1.01/0.0/0.0/16_019/0000797, L.Š., M.F.), CzeCOS (grant no. LM2015061, L.F., L.Š., M.F., N.K.), Swedish Research Council FORMAS (2016-01289, M.P.; 942-2015-49, J.C.) and University of Padua (CDPA148553, 2014, A.Pi.)

Acknowledgements. The authors thank all site collaborators, the Drought 2018 Task Force and the Ecosystem Thematic Centre of the ICOS Research Infrastructure for data provision, as well as two anonymous referees and guest editor W. Kutsch for suggestions that greatly helped to improve the manuscript, and senior editor Helen Eaton for multiple support during the revision and publication process.

References

1. Ciais P *et al.* 2005 Europe-wide reduction in primary productivity caused by the heat and drought in 2003. *Nature* **437**, 529–533. (doi:10.1038/nature03972)
2. Reichstein M *et al.* 2007 Reduction of ecosystem productivity and respiration during the European summer 2003 climate anomaly: a joint flux tower, remote sensing and modelling analysis. *Glob. Change Biol.* **13**, 634–651. (doi:10.1111/j.1365-2486.2006.01224.x)
3. Lorenzini G, Nali C, Pellegrini E. 2014 Summer heat waves, agriculture, forestry and related issues: an introduction (Editorial). *Agrochimica* **58**, 3–19.
4. Copernicus Climate Change Service. 2019 European State of the Climate 2018. See https://climate.copernicus.eu/ESOTC/2018.
5. Copernicus Climate Change Service. 2020 European State of the Climate 2019. See https://climate.copernicus.eu/ESOTC/2019.
6. Gourlez de la Motte L *et al.* 2020 Non-stomatal processes reduce gross primary productivity in temperate forest ecosystems during severe edaphic drought. *Phil. Trans. R. Soc. B* **375**, 20190527. (doi:10.1098/rstb.2019.0527)
7. Teuling AJ *et al.* 2010 Contrasting response of European forest and grassland energy exchange to heatwaves. *Nat. Geosci.* **3**, 722–727. (doi:10.1038/ngeo950)
8. Swinbank WC. 1951 The measurement of vertical transfer of heat and water vapor by eddies in the lower atmosphere. *J. Meteorol.* **8**, 135–145. (doi:10.1175/1520-0469(1951)008<0135:tmovto>2.0.co;2)
9. Drought 2018 Team and ICOS Ecosystem Thematic Centre 2020. Drought-2018 ecosystem eddy covariance flux product for 52 stations in FLUXNET-Archive format. (doi:10.18160/YVR0-4898)
10. Franz D *et al.* 2018 Towards long-term standardised carbon and greenhouse gas observations for monitoring Europe's terrestrial ecosystems: a review. *Int. Agrophys.* **32**, 439. (doi:10.1515/intag-2017-0039)
11. Mauder M, Cuntz M, Drüe C, Graf A, Rebmann C, Schmid H-P, Schmidt M, Steinbrecher R. 2013 A quality assessment strategy for long-term eddy-covariance measurements. *Agric. For. Meteorol.* **169**, 122–135. (doi:10.1016/j.agrformet.2012.09.006)
12. Sabbatini S *et al.* 2018 Eddy covariance raw data processing for CO2 and energy fluxes calculation at

ICOS ecosystem stations. *Int. Agrophys.* **32**, 495. (doi:10.1515/intag-2017-0043)

13. Wutzler T, Lucas-Moffat A, Migliavacca M, Knauer J, Sickel K, Sigut L, Menzer O, Reichstein M. 2018 Basic and extensible post-processing of eddy covariance flux data with REddyProc. *Biogeosciences* **15**, 5015–5030. (doi:10.5194/bg-15-5015-2018)
14. Blanken PD, Black TA, Yang PC, Neumann HH, Nesic Z, Staebler R, den Hartog G, Novak MD, Lee X. 1997 Energy balance and canopy conductance of a boreal aspen forest: partitioning overstory and understory components. *J. Geophys. Res. Atmos.* **102**, 28 915–28 927. (doi:10.1029/97jd00193)
15. Meyers TP, Hollinger SE. 2004 An assessment of storage terms in the surface energy balance of maize and soybean. *Agric. For. Meteorol.* **125**, 105–115. (doi:10.1016/j.agrformet.2004.03.001)
16. Eshonkulov R, Poyda A, Ingwersen J, Wizemann HD, Weber TKD, Kremer P, Hogy P, Pulatov A, Streck T. 2019 Evaluating multi-year, multi-site data on the energy balance closure of eddy-covariance flux measurements at cropland sites in southwestern Germany. *Biogeosciences* **16**, 521–540. (doi:10.5194/bg-16-521-2019)
17. Oncley SP *et al.* 2007 The energy balance experiment EBEX-2000. Part I: overview and energy balance. *Bound.-Layer Meteor.* **123**, 1–28. (doi:10.1007/s10546-007-9161-1)
18. Leuning R, van Gorsel E, Massman WJ, Isaac PR. 2012 Reflections on the surface energy imbalance problem. *Agric. For. Meteorol.* **156**, 65–74. (doi:10.1016/j.agrformet.2011.12.002)
19. Allen RG, Pereira LS, Raes D, Smith M. 1998 *Crop evapotranspiration: guidelines for computing crop water requirements*, 300 p. Rome, Italy: FAO.
20. Thornthwaite CW. 1948 An approach toward a rational classification of climate. *Geogr. Rev.* **38**, 55–94. (doi:10.2307/210739)
21. Buras A, Rammig A, Zang CS. 2019 Quantifying impacts of the drought 2018 on European ecosystems in comparison to 2003. *Biogeosci. Discuss.* **2019**, 1–23. (doi:10.5194/bg-2019-286)
22. Vicente-Serrano SM, Begueria S, Lorenzo-Lacruz J, Camarero JJ, Lopez-Moreno JI, Azorin-Molina C, Revuelto J, Moran-Tejeda E, Sanchez-Lorenzo A. 2012 Performance of drought indices for ecological, agricultural, and hydrological applications. *Earth Interact.* **16**, 1–27. (doi:10.1175/2012ei000434.1))
23. Bastos A *et al.* 2020 Direct and seasonal legacy effects of the 2018 heat wave and drought on European ecosystem productivity. *Science Advances* **6**, eaba2724. (doi:10.1126/sciadv.aba2724)
24. Vicente-Serrano SM, Begueria S. 2020 SPEI Global drought monitor. See https://spei.csic.es/map/maps.html.
25. Stoy PC *et al*. 2013 A data-driven analysis of energy balance closure across FLUXNET research sites: the role of landscape scale heterogeneity. *Agric. For. Meteorol.* **171–172**, 137–152. (doi:10.1016/j.agrformet.2012.11.004).
26. Wilson K *et al.* 2002 Energy balance closure at FLUXNET sites. *Agric. For. Meteorol.* **113**, 223–243. (doi:10.1016/s0168-1923(02)00109-0)
27. Foken T, Aubinet M, Finnigan JJ, Leclerc MY, Mauder M, Paw UKT. 2011 Results of a panel discussion about the energy balance closure correction for trace gases. *Bull. Am. Meteorol. Soc.* **92**, ES13–ES18. (doi:10.1175/2011BAMS3130.1)
28. Budyko MI. 1974 *Climate and life*. New York, NY: Academic Press.
29. Williams CA *et al.* 2012 Climate and vegetation controls on the surface water balance: synthesis of evapotranspiration measured across a global network of flux towers. *Water Resour. Res.* **48**, W06523. (doi:10.1029/2011wr011586)
30. Nijp JJ, Metselaar K, Limpens J, Bartholomeus HM, Nilsson MB, Berendse F, van der Zee S. 2019 High-resolution peat volume change in a northern peatland: spatial variability, main drivers, and impact on ecohydrology. *Ecohydrology* **12**, 17. (doi:10.1002/eco.2114)
31. Wolf S *et al.* 2013 Contrasting response of grassland versus forest carbon and water fluxes to spring drought in Switzerland. *Environ. Res. Lett.* **8**, 12. (doi:10.1088/1748-9326/8/3/035007)
32. Teuling AJ *et al.* 2013 Evapotranspiration amplifies European summer drought. *Geophys. Res. Lett.* **40**, 2071–2075. (doi:10.1002/grl.50495)
33. Kabat P *et al*. 2004 *Vegetation, water, humans and the climate: a new perspective on an Interactive system*. Dordrecht, The Netherlands: Springer.
34. Betts RA. 2000 Offset of the potential carbon sink from boreal forestation by decreases in surface albedo. *Nature* **408**, 187–190. (doi:10.1038/35041545)
35. Rotenberg E, Yakir D. 2010 Contribution of semi-arid forests to the climate system. *Science* **327**, 451–454. (doi:10.1126/science.1179998)
36. Ramonet M *et al.* 2020 The fingerprint of the summer 2018 drought in Europe on ground-based atmospheric CO_2 measurements. *Phil. Trans. R. Soc. B* **375**, 20190513. (doi:10.1098/rstb.2019.0513)
37. Thompson RL *et al.* 2020 Changes in net ecosystem exchange over Europe during the 2018 drought based on atmospheric observations. *Phil. Trans. R. Soc. B* **375**, 20190512. (doi:10.1098/rstb.2019.0512)
38. Wohlfahrt G *et al*. 2018 Sun-induced fluorescence and gross primary productivity during a heat wave. *Sci. Rep*. **8**, 9. (doi:10.1038/s41598-018-32602-z)
39. Stoy PC *et al.* 2019 Reviews and syntheses: turning the challenges of partitioning ecosystem evaporation and transpiration into opportunities. *Biogeosciences* **16**, 3747–3775. (doi:10.5194/bg-16-3747-2019)
40. Beer C *et al.* 2009 Temporal and among-site variability of inherent water use efficiency at the ecosystem level. *Global Biogeochem. Cycles* **23**, 13. (doi:10.1029/2008gb003233)